J Mater Sci (2008) 43:1366–1375
DOI 10.1007/s10853-007-2288-0

Preparation and properties of fluoroalkyl end-capped oligomer/fluoresceins nanocomposites

Kazuo Sasazawa · Yuko Yamada · Hideo Sawada

Received: 27 July 2007 / Accepted: 31 October 2007 / Published online: 12 December 2007

Abstract Self-assembled fluorinated oligomeric aggregates formed by fluoroalkyl end-capped *N*-(1,1-dimethyl-3-oxobutyl)acrylamide oligomers, *N,N*-dimethylacrylamide oligomers, and acrylic acid oligomers in methanol could recognize selectively fluoresceins as guest molecules to form a new class of fluorinated aggregates/fluoresceins nanocomposites. These fluorinated fluoresceins nanocomposites were found to exhibit an extraordinarily enhanced light absorption ($\lambda_{\max}$: ca. 440 nm) compared to that (λ_{maxs}: 452 and 480 nm) of the parent fluorescein in the absence of fluorinated aggregates. On the other hand, fluoroalkyl end-capped 2-carboxyethyl acrylate oligomers, which possess no aggregate characteristic in methanol solutions, could not afford such an enhanced light absorption peak under similar conditions. Not only fluorescein but also fluorescein derivatives such fluoresceinamine, carboxyfluorescein, and fluorescein isothiocyanate afforded similar enhanced narrow absorption peaks under similar conditions. Naphthofluorescein was also encapsulated into these fluorinated oligomeric aggregate cores to afford fluorinated aggregates/naphthofluorescein composites, and these fluorinated naphthofluorescein composites afforded an extremely enhanced narrow absorption peak around 520 nm.

Introduction

Considerable interest has been devoted in recent years to block copolymers containing fluoroalkyl groups owing to exhibiting the low surface energy and the self-assembled polymeric aggregates resembling micelle in aqueous and organic media, which cannot be achieved in the corresponding randomly fluorinated copolymers [1]. From the viewpoints of increasing interests for the preparation and applications of fluorinated block copolymers, it is very important to develop new preparative methods of fluorinated block copolymers [2]. In fact, we have already demonstrated that two fluoroalkyl end-capped triblock-type cooligomers [R_F–$(M)_n$–R_F] can be prepared by the oligomerizations of fluoroalkanoyl peroxides [$(R_FCOO)_2$] with radical polymerizable monomers (M) such as acrylic acid and acryloylmorpholine [3]. In these fluoroalkyl end-capped oligomers, in particular, amphiphilic fluoroalkyl end-capped oligomers are attractive materials, because they exhibit various unique properties such as high solubility, surface active properties, biological activities, and nanometer size-controlled self-assembled molecular aggregates which cannot be achieved by the corresponding non-fluorinated and randomly fluoroalkylated ones [4]. For example, self-assembled fluorinated oligomeric aggregates formed by fluoroalkyl end-capped acryloylmorpholine oligomers could interact with fullerene, carbon nanotubes, nanodiamond, and metal particles as guest molecules in aqueous and organic media to afford nanometer size-controlled fluorinated aggregates/these guest molecules composites [5]. These fluorinated nanocomposites should have high potential for new nanomaterials possessing a surface-active characteristic imparted by fluorine. From the viewpoint of the higher applicable potential in material syntheses, the development of the preparation of novel

---

K. Sasazawa
Central R&D Laboratories, Taiyo Yuden Co., Ltd.,
8-1 Sdakae-cho, Takasaki, Gunma 370-8522, Japan

Y. Yamada · H. Sawada (✉)
Department of Frontier Materials Chemistry, Graduate School
of Science and Technology, Hirosaki University, Bunkyo-cho,
Hirosaki 036-8561, Japan
e-mail: hideosaw@cc.hirosaki-u.ac.jp

organic nanomaterials is much interesting. In fact, much attention has been focused on the systematic research works through the preparation of nanoparticles by a precipitation method [6]. Therefore, it is in particular interest to explore the novel synthetic systems of organic nanomaterials possessing a unique characteristic imparted by fluorine using organofluorine compounds, especially fluoroalkyl end-capped oligomers. In our continuing effort to design and develop the preparation of organic nanocomposites by the use of fluoroalkyl end-capped oligomers, we discovered that self-assembled fluorinated oligomeric aggregates formed by fluoroalkyl end-capped oligomers in methanol can interact selectively with fluorescein as guest molecules to form a new class of fluorinated aggregates/fluorescein nanocomposites with a mean diameter of 46 nm, leading to the dramatic increase of the light absorption compared to that of the parent fluorescein [7]. We now give a full account of the preparation and properties of fluoroalkyl end-capped oligomers/fluoresceins nanocomposites, with emphasis on light absorption of these fluorinated nanocomposites.

Experimental

Measurements

Molecular weights were measured using a Shodex DS-4 (pomp, Tokyo, Japan) and Shodex RI-71 (detector) gel permeation chromatography (GPC) calibrated with polystyrene standard using tetrahydrofuran (THF) as the eluent. NMR spectra and Fourier-transform infrared (FTIR) spectra were measured using JEOL JNM-400 (400 MHz) FT NMR SYSTEM (Tokyo, Japan) and Shimadzu FTIR-8400 FTIR spectrophotometer (Kyoto, Japan), respectively. Dynamic light-scattering (DLS) and static light-scattering (SLS) measurements were measured using Otsuka Electronics DLS-7000 HL (Tokyo, Japan). Ultraviolet–visible (UV–vis) spectra were measured using Shimadzu UV-1600 UV–vis spectrophotometer (Kyoto, Japan). The surface tensions of aqueous methanol solutions of the fluoroalkyl end-capped oligomers were measured at 30 °C by the drop weight-type surface tensiometer (Ver. 1.00 DVS-2000 system, Yamashita Giken Co., Ltd., Tokushima, Japan). The formation of the nanocomposites was observed from SEM (scanning electron microscope: JEOL JSM-5300, Tokyo, Japan).

Materials

Acrylic acid (ACA) and *N*,*N*-dimethylacrylamide (DMAA) were used as received from Toagosei Co., Ltd. (Tokyo, Japan) and Kohjin Co., Ltd. (Tokyo, Japan), respectively. *N*-(1,1-dimethyl-3-oxobutyl)acrylamide (DOBAA) was used as received Kyowa Hakko Kogyou Co., Ltd. (Tokyo, Japan). Fluorescein, uranine, fluoresceinamine, carboxyfluorescein, fluorescein diacetate, fluorescein isothiocyanate, and methyl orange were purchased from Wako Pure Chemical Industries, Ltd. (Osaka, Japan). Indigo carmine, tropaeolin O, lucigenin, eriochrome black T, ethidium bromide, aminophthalic acid, methyl red, 4-methylumbelliferone, phenyl acridine-9-carboxylate, 4-hydroxyazobenzene-4′-sulfonic acid, rhodamine B, methylene blue, acridine hydrochloride, methyl orange, 4-hydroxyazobenzene-4′-sulfonic acid sodium salt, and acriflavine hydrochloride were purchased from Tokyo Kasei Kogyou Co., Ltd. (Tokyo, Japan). 2-Carboxyethyl acrylate (CEA) and naphthofluorescein were purchased from Sigma-Aldrich Japan Corp. (Tokyo, Japan). Fluoroalkyl end-capped DOBAA, DMAA, and ACA oligomers were prepared by the methods described in the literatures [3a, 3c, 8].

Synthesis of fluoroalkyl end-capped CEA oligomers

Perfluoro-2-methyl-3-oxahexanoyl peroxide (3.1 mmol) in AK-225 (1:1 mixed solvents of 1,1-dichloro-2,2,3,3,3-pentafluoropropane and 1,3-dichloro-1,2,2,3,3-pentafluoropropane: 25 g) was added to a mixture of CEA (16.9 mmol) and AK-225 (180 g). The solution was stirred at 45 °C for 5 h under nitrogen. After evaporating the solvent, the obtained crude products were reprecipitated from the methanol—AK-225 system to give an α,ω-bis(perfluoro-1-methyl-2-oxapentylated) CEA oligomer (2.21 g). This oligomer exhibited the following spectra characteristics:

IR (ν/cm^{-1}) 3080 (OH), 1732 (C=O), 1242 (CF_2); ^{1}H NMR ($CDCl_3$) δ 1.42–2.02 (CH_2), 2.23–2.80 (CH, CH_2), 4.18–4.41 (CH_2).

The other product obtained exhibited the following spectra characteristics.

R_F–(CEA)$_n$–R_F; R_F = $CF(CF_3)OCF_2CF(CF_3)OC_3F_7$: IR ($\nu$/cm^{-1}) 3110 (OH), 1732 (C=O), 1242 (CF_2); ^{1}H NMR ($CDCl_3$) δ 1.43–2.04 (CH_2), 2.23–2.80 (CH, CH_2), 4.17–4.43 (CH_2).

Preparation of R_F–(DOBAA)$_n$–R_F/fluorescein nanocomposites

To a methanol solution (2 mL) of 4 g/dm^3 R_F–(CEA)$_x$–(DMAA)$_y$–R_F was added a methanol solution (2 mL) of

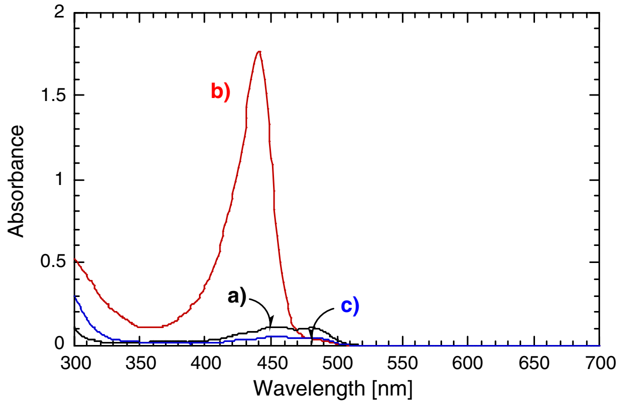

Fig. 1 UV–vis spectra of methanol solution of fluorescein in the presence of R_F–(DOBAA)$_n$–R_F oligomer. (**a**) Fluorescein (0.1 mmol/dm^3) in MeOH. (**b**) R_F–(DOBAA)$_n$–R_F [R_F = $CF(CF_3)OC_3F_7$; Mn = 3,710] (2 g/dm^3)–fluorescein (0.1 mmol/dm^3) in MeOH. (**c**) –(DOBAA)$_n$– [Mn = 5,820] (2 g/dm^3)–fluorescein (0.1 mmol/dm^3) in MeOH

fluorescein (0.2 mmol). The mixture was stirred with a magnetic stirring bar at room temperature for 1 h to afford R_F–(DOBAA)$_n$–R_F/fluorescein nanocomposites. The formation of R_F–(DOBAA)$_n$–R_F/fluorescein nanocomposites in the methanol solution was confirmed by the use of UV–vis spectra (λ_{max}: ca. 440 nm), and the result was shown in Fig. 1. Other fluorinated oligomers/fluoresceins and naphthofluorescein nanocomposites were prepared under similar conditions, and the formation of these nanocomposites was spectrophotometrically confirmed.

Results and discussion

UV–vis spectra of methanol solution of fluorescein (0.1 mmol/dm^3) show absorption band at 452 nm (enol form) and 480 nm (keto form); however, these absorption bands completely disappeared by the addition of fluoroalkyl end-capped *N*-(1,1-dimthyl-3-oxobutyl)acrylamide oligomer [R_F–(DOBAA)$_n$–R_F] and very interestingly, an intense narrow absorption band was newly observed at 440 nm as shown in Fig. 1.

In contrast, such absorption band was not observed in the presence of the corresponding non-fluorinated DOBAA oligomer, and UV–vis spectra showed the same two absorption bands as with the parent fluorescein. This intense narrow absorption band in Fig. 1 is also evident from the difference in colors of methanol solutions of the parent fluorescein (transparent colorless solution: (a) in Fig. 1), fluorescein/–(DOBAA)$_n$– oligomer (transparent colorless solution: (c) in Fig. 1), and fluorescein/R_F–(DOBAA)$_n$–R_F (transparent yellow-colored solution: (b) in Fig. 1).

Additionally, we tried to measure the UV–vis spectra of a variety of fluorescein derivatives such as uranine, fluoresceinamine, carboxyfluorescein, fluorescein diacetate, and fluorescein isothiocyanate (see Chart 1) under similar conditions, and the results were shown in Table 1.

As shown in Table 1, each absorption band (λ_{maxs}: 452 and 480 nm) of the parent fluorescein derivatives was completely disappeared in the presence of R_F–(DOBAA)$_n$–R_F oligomer, and intense narrow absorption bands around 440 nm were newly observed in these fluorescein derivatives.

Interestingly, the wavelength of the ultraviolet intense narrow absorption for fluoresceinamine was found to be slightly blue-shifted from 440 (fluorescein) to 435 nm; in contrast, it was demonstrated that in the cases of fluorescein isothiocyanate and carboxyfluorescein, these wavelengths were slightly red-shifted to 442 and 443 nm, respectively.

In particular interest, uranine and fluorescein diacetate, in which –OH groups are substituted for –ONa and –OC(=O)Me, respectively, were not able to afford such intense narrow absorption bands around 440 nm, and the ratio of absorbance [$A_{oligomer}$(ca. 440 nm)/A(ca. 450 nm)] [the ratios of the absorbance around 440 nm based on that (around 450 nm) of the parent fluorescein] became significantly decrease. On the other hand, fluorescein and

Chart 1 Fluorescein derivatives

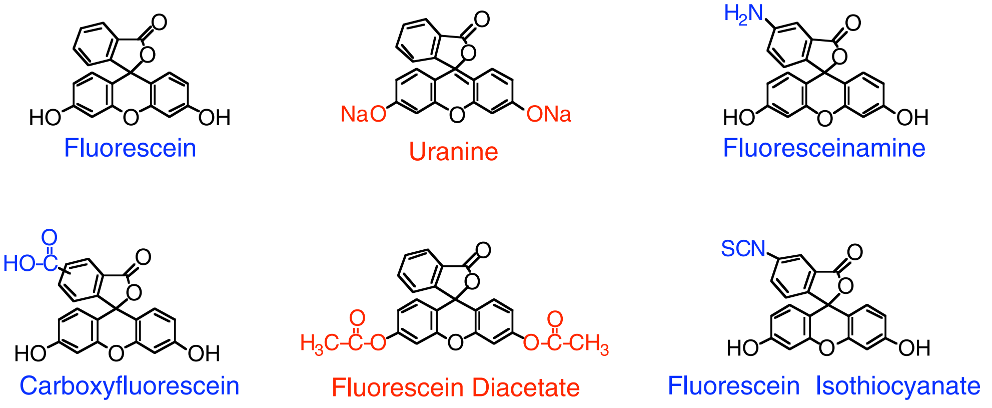

Table 1 Absorbance (A) of fluorescein derivatives in methanol in the presence of 2.0 g/dm^3 R_F–(DOBAA)$_n$–R_F [$R_F = CF(CF_3)OC_3F_7$; Mn = 3,710]

Fluorescein derivatives	In the absence of oligomer	In the presence of oligomer	
	λ_{max} (nm) [A]	λ_{max} (nm) [A]	$A_{oligomer}$(ca.440 nm)/A(ca.450 nm)
Fluorescein (0.1 mmol/dm^3)	452 [0.101] 480 [0.095]	440 [1.467]	14.5
Uranine (0.03 mmol/dm^3)	457 [0.512] 489 [0.678]	440 [0.392]	0.8
Fluoresceinamine (0.10 mmol/dm^3)	452 [0.204] 479 [0.190]	435 [2.834]	13.9
Fluorescein isothiocyanate (0.20 mmol/dm^3)	442 [0.601]	442 [2.834]	4.7
Carboxyfluorescein (0.10 mmol/dm^3)	443 [0.569]	443 [1.366]	2.4
Fluorescein diacetate (1.0 mmol/dm^3)	450 [0.081] 477 [0.068]	440 [0.108]	1.3

fluoresceinamine had remarkably higher values (14.5 and 13.9), indicating that fluorinated self-assembled oligomeric aggregates formed by R_F–(DOBAA)$_n$–R_F oligomer in methanol could provide suitable host moieties to recognize selectively fluorescein derivatives bearing hydroxyl groups as guest molecules.

A similar result was obtained in the case of naphthofluorescein, and an extremely intense narrow absorption around 520 nm was observed in the presence of R_F–(DOBAA)$_n$–R_F oligomer, although such absorption band was not observed at all in the presence of the corresponding nonfluorinated DOBAA oligomer and in the absence of oligomer (see Fig. 2). Calcein bearing two bulky substituents on aromatic nuclei (see Chart 2), which is one of fluorescein derivatives, failed to exhibit the enhanced absorption band around 440 nm, suggesting that calcein is not likely to interact with fluorinated molecular aggregates as guest molecule due to the steric hindrance.

Traditional organic dyes such as indigo carmine, tropaeolin O, lucigenin, eriochrome black T, ethidium bromide, aminophthalic acid, methyl red, 4-methylumbelliferone, phenyl acridine-9-carboxylate, 4-hydroxyazobenzene-4′-sulfonic acid, rhodamine B, methylene blue, acridine hydrochloride, methyl orange, 4-hydroxyazobenzene-4′-sulfonic acid sodium salt, and acriflavine hydrochloride, which possess no fluorescein's units, were not able to interact with fluorinated oligomeric aggregates at all, and only the original absorption bands related to parent organic dyes were observed.

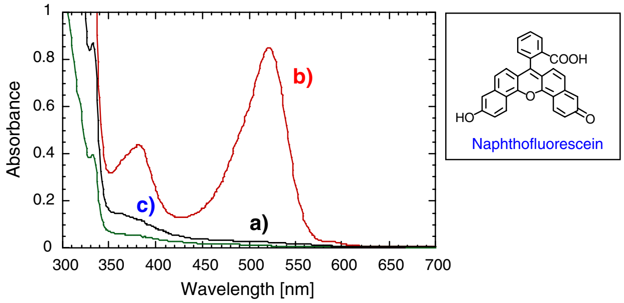

Fig. 2 UV–vis spectra of methanol solution of naphthofluorescein in the presence of R_F–(DOBAA)$_n$–R_F oligomer. (**a**) Naphthofluorescein (0.25 mmol/dm^3) in MeOH. (**b**) R_F–(DOBAA)$_n$–R_F (2 g/dm^3)–naphthofluorescein (0.25 mmol/dm^3) in MeOH. (**c**) –(DOBAA)$_n$–(2 g/dm^3)–naphthofluorescein (0.25 mmol/dm^3) in MeOH

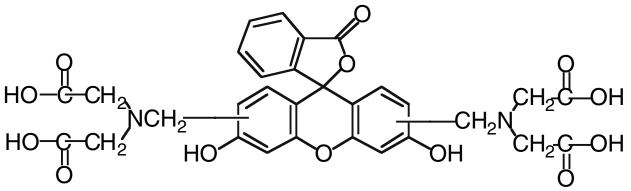

Chart 2 Calcein

To calculate the maximum number of fluorescein that could occupy the fluorinated aggregate core, we have studied on the relationship between the absorbance of fluorescein and the concentrations of fluorescein in the presence of fluorinated oligomers, and the results were shown in Fig. 3.

As shown in Fig. 3, the absorbance of 440 nm in the presence of R_F–(DOBAA)$_n$–R_F oligomer increased remarkably with increasing the concentration of fluorescein, and the almost constant values were obtained above 0.2 mmol/dm^3. On the other hand, the absorbance of 452 nm related to the parent fluorescein (enol isomer) in the presence of –(DOBAA)$_n$– oligomer increased slightly with increasing the concentration of fluorescein. This experimental result shows that 2 g/dm^3 oligomer could interact with 0.2 mmol/dm^3 fluorescein. Thus, one mole of R_F–(DOBAA)$_n$–R_F oligomer could interact with ca. 0.37 mol of fluorescein, indicating that fluorinated

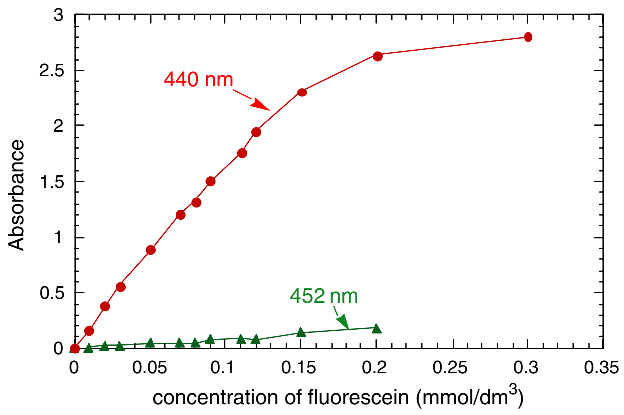

Fig. 3 Relationship between the absorbance of fluorescein and the concentrations of fluorescein in the presence of oligomers (2 g/dm^3) in methanol. (●) R_F–(DOBAA)$_n$–R_F; R_F = CF(CF$_3$)OC$_3$F$_7$ (Mn = 3,710), (▲) –(DOBAA)$_n$– (Mn = 5,820)

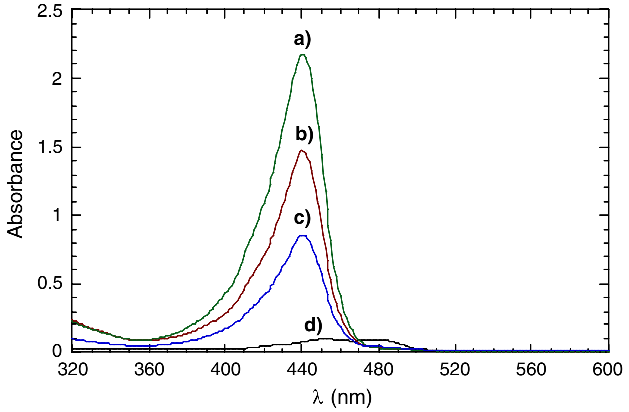

Fig. 4 UV–vis spectra of methanol solutions of 0.10 mmol/dm^3 fluorescein in the presence of fluoroalkyl end-capped oligomers (concentration of oligomer: 2 g/dm^3). (**a**) R_F–(DMAA)$_n$–R_F; R_F = CF(CF$_3$)OC$_3$F$_7$ (Mn = 4,820). (**b**) R_F–(DOBAA)$_n$–R_F; R_F = CF(CF$_3$)OC$_3$F$_7$ (Mn = 3,710). (**c**) R_F–(ACA)$_n$–R_F; R_F = CF(CF$_3$)OC$_3$F$_7$ (Mn = 5,220). (**d**) 0.10 mmol/dm^3 fluorescein in the absence of oligomer

oligomeric aggregate could occupy around 3 fluorescein molecules per aggregate core (see Scheme 1); because this fluorinated molecular aggregate is considered to consist of around 8 fluorinated oligomeric molecules since the molecular weight of the aggregates formed by the fluorinated oligomer determined by the static light scattering measurements and the molecular weight of the fluorinated oligomer determined by GPC (gel permeation chromatography) measurements are 30,310 and 3,710, respectively.

We tried to measure the UV–vis spectra of fluorescein by the use of not only fluorinated DOBAA oligomers but also other fluorinated oligomers such as fluoroalkyl end-capped acrylic acid oligomers [R_F–(CH$_2$CHCOOH)$_n$–R_F (R_F–(ACA)$_n$–R_F)] and *N,N*-dimethylacrylamide oligomers [R_F–(CH$_2$CHCONMe$_2$)$_n$–R_F (R_F–(DMAA)$_n$–R_F)] under similar conditions (see Fig. 4 and Table 2).

As shown in Fig. 4 and Table 2, not only fluorinated DOBAA oligomer but also fluorinated ACA and DMAA oligomers gave a similar intense narrow absorption peak around 440 nm, although the corresponding non-fluorinated oligomers failed to exhibit such enhanced absorption peaks. The interaction of R_F–(ACA)$_n$–R_F oligomer with fluorescein was found to become weaker compared to those of R_F–(DOBAA)$_n$–R_F oligomer and R_F–(DMAA)$_n$–R_F oligomer. We could have the highest enhanced absorption band (the ratio of absorbance [A_{oligomer}(ca. 440 nm)/A(ca. 450 nm)] [the ratios of the absorbance around 440 nm in the presence of oligomer based on that (around 450 nm) of the parent fluorescein]: 21.5) in the case of R_F–(DMAA)$_n$–R_F oligomer.

Fluorinated DMAA and ACA oligomers were also found to afford the same intense narrow absorption peaks related to naphthofluorescein around 520 nm as with fluorinated DOBAA oligomer (see Table 3). The ratio of the absorbance [A_{oligomer}(ca. 520 nm)/A(520 nm): the ratios of the absorbance around 520 nm in the presence of oligomers based on that (520 nm) of the parent naphthofluorescein under the same conditions] was found to increase effectively in the presence of fluorinated

Scheme 1 Interaction of fluorinated oligomeric aggregates with fluorescein

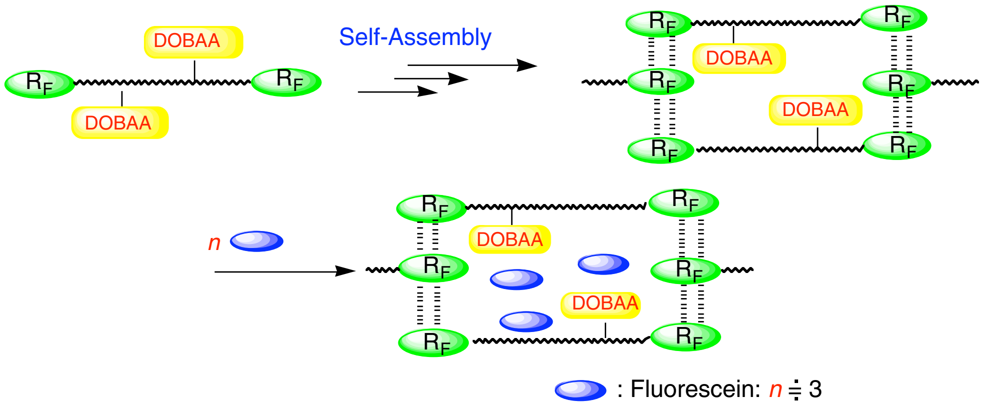

Table 2 Absorbance (*A*) of 0.10 mmol/dm^3 fluorescein in methanol in the presence of a variety of fluorinated oligomers [2.0 g/dm^3]

Oligomer	λ_{max} (nm) [*A*]	$A_{oligomer}$(ca.440 nm)/*A*(ca.450 nm)
No oligomer	452 [0.101], 480 [0.095]	0
R_F–(DOBAA)$_n$–R_F		
R_F =CF(CF$_3$)OC$_3$F$_7$ (Mn = 3,710)	440 [1.467]	14.5
R_F = CF(CF$_3$)OCF$_2$CF(CF$_3$)OCF$_2$CF(CF$_3$)OC$_3$F$_7$ (Mn = 9,390)	440 [1.621]	16.0
R_F = C$_3$F$_7$ (Mn = 8,090)	440 [1.167]	11.6
R_F = non-fluorinated; Mn = 5,820]	452 [0.083], 480 [0.077]	0
R_F–(DMAA)$_n$–R_F		
R_F = CF(CF$_3$)OC$_3$F$_7$ (Mn = 4,820)	440 [2.173]	21.5
R_F–(ACA)$_n$–R_F		
R_F = CF(CF$_3$)OC$_3$F$_7$ (Mn = 5,220)	440 [0.854]	8.5
R_F = CF(CF$_3$)OCF$_2$CF(CF$_3$)OC$_3$F$_7$ (Mn = 4,250)	441 [0.904]	9.0

oligomers, and an extremely higher ratio (200.3) was obtained in the case of fluorinated DMAA oligomer. In contrat, the absorbance ratio of the corresponding non-fluorinated DMAA oligomer was extremely lower (3.1: see Table 3).

We have measured the size of fluorinated oligomeric aggregates formed by R_F–(DMAA)$_n$–R_F [2 g/dm^3: R_F = CF(CF$_3$)OC$_3$F$_7$] in methanol solutions at 30 °C by the dynamic light scattering (DLS) measurements. DLS measurements shows that R_F–(DMAA)$_n$–R_F oligomer can form the nanometer size-controlled fluorinated molecular aggregates (84.8 ± 9.6 nm) in methanol solution. The size of fluorinated aggregates was found to increase from 84.8 nm to 114.1 ± 12.1 nm by the composization with fluorescein (0.1 mol/dm^3). This finding suggests that fluorescein should be tightly encapsulated into the fluorinated oligomeric aggregate cores to afford the fluorinated oligomer/fluorescein nanocomposites.

Unexpectedly, as shown in Fig. 5, fluoroalkyl end-capped 2-carboxyethyl acrylate oligomers [R_F–(CH$_2$CHC(=O)OCH$_2$CH$_2$C(=O)OH)$_n$–R_F (R_F–(CEA)$_n$–R_F)], which were prepared by the reactions of fluoroalkanoyl peroxides with the corresponding monomer, were not able to afford newly a similar intense narrow absorption peak around 440 nm to that of R_F–(ACA)$_n$–R_F oligomer, and almost the same absorption bands as with the parent fluorescein were observed. A similar result was obtained in the case of the corresponding non-fluorinated CEA oligomer [–(CEA)$_n$–]. This finding would results from that R_F–(CEA)$_n$–R_F oligomers have a poor surface active characteristic due to the electrostatic repulsion between the carboxyl groups in

Table 3 Absorbance (*A*) of 0.25 mmol/dm^3 Naphthofluorescein in methanol in the presence of a variety of fluorinated oligomers [2.0 g/dm^3]

Oligomer	λ_{max} (nm) [*A*]	$A_{oligomer}$(ca.521 nm)/*A*
No oligomer	521 [0.009]	
R_F–(DOBAA)$_n$–R_F		
R_F = CF(CF$_3$)OC$_3$F$_7$ (Mn = 3,710)	521 [0.848]	94.2
–(DOBAA)$_n$– (Mn = 5,820)	521 [0.024]	2.7
R_F–(DMAA)$_n$–R_F		
R_F = CF(CF$_3$)OC$_3$F$_7$ (Mn = 4,820)	521 [1.803]	200.3
–(DMAA)$_n$– (Mn = 22,550)	521 [0.028]	3.1
R_F–(ACA)$_n$–R_F		
R_F = CF(CF$_3$)OC$_3$F$_7$ (Mn = 5,220)	521 [0.620]	68.9
–(ACA)$_n$– (Mn = 6,520)	521 [0.033]	3.7

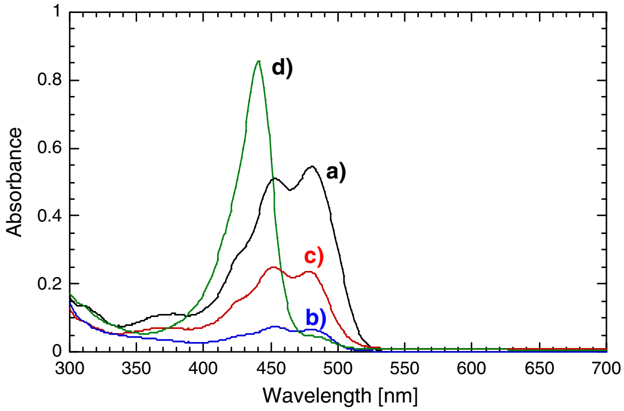

Fig. 5 UV–vis spectra of methanol solutions of fluorescein in the presence of R_F–(CEA)$_n$–R_F and R_F–(ACA)$_n$–R_F oligomer. (**a**) Fluorescein (0.1 mmol/dm^3) in MeOH. (**b**) R_F–(CEA)$_n$–R_F (2 g/dm^3)–fluorescein (0.1 mmol/dm^3) in MeOH. (**c**) –(CEA)$_n$– (2 g/dm^3)–fluorescein (0.1 mmol/dm^3) in MeOH. (**d**) R_F–(ACA)$_n$–R_F (2 g/dm^3)–fluorescein (0.1 mmol/dm^3) in MeOH

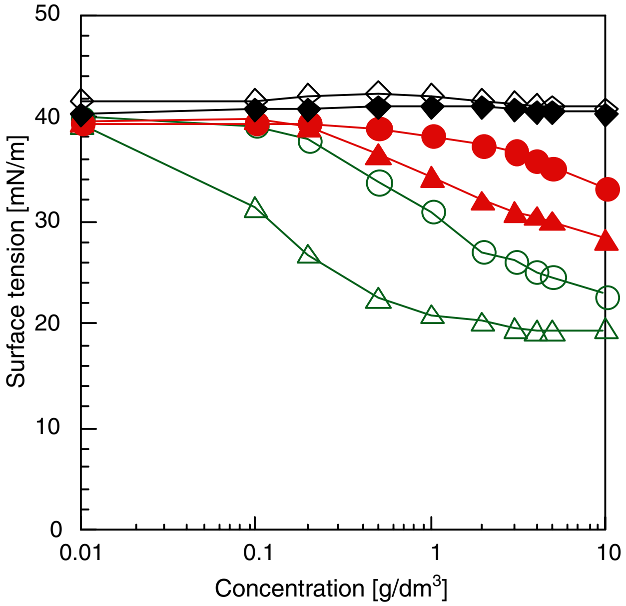

Fig. 6 Surface tension of aqueous methanol solutions [H_2O/MeOH = 1/1 (volume)] of fluoroalkyl end-capped CEA and ACA oligomers at 30 °C. (◇) –$(\mathrm{ACA})_n$– [Mn = 6,520], (○) $\mathrm{R_F}$–$(\mathrm{ACA})_n$–$\mathrm{R_F}$; $\mathrm{R_F} = \mathrm{CF(CF_3)OC_3F_7}$ [Mn = 5,220], (△) $\mathrm{R_F}$–$(\mathrm{ACA})_n$–$\mathrm{R_F}$; $\mathrm{R_F} = \mathrm{CF(CF_3)OCF_2CF(CF_3)OC_3F_7}$ [Mn = 4,250], (◆) –$(\mathrm{CEA})_n$–, (●) $\mathrm{R_F}$–$(\mathrm{CEA})_n$–$\mathrm{R_F}$; $\mathrm{R_F} = \mathrm{CF(CF_3)OC_3F_7}$ [Mn = 4,620], (▲) $\mathrm{R_F}$–$(\mathrm{CEA})_n$–$\mathrm{R_F}$; $\mathrm{R_F} = \mathrm{CF(CF_3)OCF_2CF(CF_3)OC_3F_7}$ [Mn = 7,300]

oligomers, quite different from fluoroalkyl end-capped acrylic acid oligomers [$\mathrm{R_F}$–$(\mathrm{CH_2CHC({=}O)OH})_n$–$\mathrm{R_F}$].

In order to clarify this result in detail, the surface properties of $\mathrm{R_F}$–$(\mathrm{CEA})_n$–$\mathrm{R_F}$ oligomers were evaluated by measuring surface tension of MeOH/H_2O (1/1 vol.) mixed solutions of these fluorinated oligomers using the drop weight method at 30 °C. We have also measured surface tension of the solutions containing the corresponding $\mathrm{R_F}$–$(\mathrm{ACA})_n$–$\mathrm{R_F}$ oligomers, for comparison. These results were shown in Fig. 6.

As shown in Fig. 6, $\mathrm{R_F}$–$(\mathrm{CEA})_n$–$\mathrm{R_F}$ oligomers were not able to reduce the surface tension of the mixed solvents, effectively, compared to the corresponding ACA oligomers. This would be due to the strong electrostatic repulsion between the carboxyl groups in $\mathrm{R_F}$–$(\mathrm{CEA})_n$–$\mathrm{R_F}$ oligomers, because these carboxyl groups were introduced into oligomeric main chains through the ester units. In contrast, we could not observe such electrostatic repulsions in $\mathrm{R_F}$–$(\mathrm{ACA})_n$–$\mathrm{R_F}$ oligomer, because the carboxyl groups in this oligomer were directly introduced into oligomeric main chains. Fluoroalkyl end-capped ACA oligomers can form the self-assembled fluorinated oligomeric aggregates with the aggregations of terminal fluoroalkyl segments in aqueous and organic media. On the other hand, it is strongly suggested that $\mathrm{R_F}$–$(\mathrm{CEA})_n$–$\mathrm{R_F}$ oligomers could not form the nanometer size-controlled molecular aggregates, due to the electrostatic repulsions between the carboxyl groups in oligomers. Thus, we have measured the molecular weights of $\mathrm{R_F}$–$(\mathrm{CEA})_n$–$\mathrm{R_F}$ oligomer [$\mathrm{R_F} = \mathrm{CF(CF_3)OCF_2CF(CF_3)OC_3F_7}$] and $\mathrm{R_F}$–$(\mathrm{ACA})_n$–$\mathrm{R_F}$ oligomer [$\mathrm{R_F} = \mathrm{CF(CF_3)OCF_2CF(CF_3)OC_3F_7}$] in methanol by the static light-scattering (SLS) measurements at 30 °C. The molecular weights of $\mathrm{R_F}$–$(\mathrm{ACA})_n$–$\mathrm{R_F}$ oligomeric aggregates determined by SLS and GPC measurements were 75,100 and 2,630, respectively. This indicates that fluorinated oligomeric aggregate formed by $\mathrm{R_F}$–$(\mathrm{ACA})_n$–$\mathrm{R_F}$ in methanol solutions are considered to consist of around 28 fluorinated oligomeric molecules. On the other hand, $\mathrm{R_F}$–$(\mathrm{CEA})_n$–$\mathrm{R_F}$ oligomers are not likely to form the self-assembled molecular aggregates, because the same values for the molecular weights of $\mathrm{R_F}$–$(\mathrm{CEA})_n$–$\mathrm{R_F}$ oligomer were obtained in the cases of SLS (MW = 7,300) and GPC (Mn = 7,300) measurements. Thus, $\mathrm{R_F}$–$(\mathrm{CEA})_n$–$\mathrm{R_F}$ oligomers should not afford an intense narrow absorption band around 440 nm related to fluorescein.

In this way, it was verified that fluoroalkyl end-capped DOBAA, DMAA and ACA oligomers were able to afford sharp intense absorptions related to fluorescein and naphthofluorescein around 440 and 520 nm, respectively; however, the corresponding nonfluorinated DOBAA, DMAA, ACA oligomers, and $\mathrm{R_F}$–$(\mathrm{CEA})_n$–$\mathrm{R_F}$ oligomers could not interact with fluorescein and naphthofluorescein at all under similar conditions.

Hitherto, cyanine-type organic dyes such 5,5′,6,6′-tetrachloro-1,1′-diethyl-3,3′-bis(4-sulfobutyl)-benzimidazolocarbo-cyanine sodium salt are well known to exhibit the J-aggregation band [8]. This band gives an intense narrow absorption band related to the interaction of “edge to edge”. H-aggregates give a broad absorption band related to the interaction of “face to face” [9]. The J aggregate band is red-shifted compared to that of the parent monomer, and this band gives an intense narrow absorption band related to the interaction of “edge to edge”. In contrast, H-aggregate band is blue-shifted, and gives a broad absorption band related to the interaction of “face to face”. However, our present result is quite different from the J-aggregate and H-aggregates. Because, fluorinated DMAA, DOBAA, and ACA oligomers can afford a blue-shifted narrow sharp absorption. Herz and Tanaka, individually, reported on the aggregation numbers (*n*) of cyanine-type organic dye, and the aggregation numbers are $n = 4$ and $n = 8$, respectively [10]. Our present result in the extraordinarily enhanced narrow blue-shifted band compared to the parent fluorescein seems to be quite different from the previously reported J band. Thus, we were interested in measuring the association number (*n*) of fluorescein according to the method reported by Herz and Tanaka et al. as shown in Fig. 7.

We have measured the UV–vis spectra of fluorescein by the use of fluoroalkyl end-capped acrylic acid oligomers

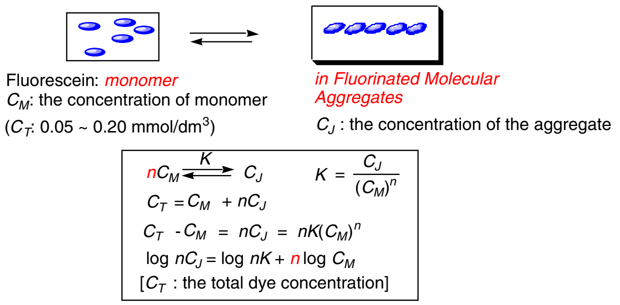

Fig. 7 Association number (n) of fluorescein in the presence of oligomer at 30 °C

(concentration of oligomer: 1.5 g/dm^3) at 30 °C, and the results were shown in Fig. 8.

As shown in Fig. 8, the narrow sharp absorption band around 440 nm could increase with the increase of the concentration of fluorescein. A similar result was obtained in the case of the concentrations of R_F–(ACA)$_n$–R_F oligomer: 0.9, 0.6, and 0.3 g/dm^3 (data not shown). We can obtain the association number (n) of fluorescein (0.05–0.20 mmol) in a variety of concentrations (0.3–1.5 g/dm^3) of R_F–(ACA)$_n$–R_F oligomer by the use of the equations in Fig. 7. The association number of fluorescein is around 1.0 in each case as shown in Table 4. This finding suggests that fluoresceins in fluorinated molecular aggregates are unable to fall into the well-known J aggregates.

Recently, An et al. reported that biphenyl ethylene derivatives in mixture of water/tetrahydrofuran was able to aggregate into nanosize controlled particles with a mean diameter of about 30–40 nm through the reprecipitation method [11]. In order to clarify this unique behavior of fluoresceins in fluorinated oligomeric aggregates, we have measured SEM (scanning electron microscopy) photographs of methanol solution of fluorescein in the presence of R_F–(DOBAA)$_n$–R_F oligomer, and the results were shown in Fig. 9.

Surprisingly, this photography shows that fluorescein nanoparticles are formed in the self-assembled fluorinated oligomeric aggregates. Fluorescein nanoparticles are very fine particles with a mean diameter of 46 nm. The insides of fluorinated molecular aggregate cores could provide the solvophobic environment, and in addition, the host moieties in these cores could recognize selectively fluoresceins as guest molecules. Thus, under such specific conditions, fluoresceins could form nanoparticles with only enol-form, especially carboxy-type tautomer in the host cores; because these nanoparticles containing –OH and –C(=O)OH groups could interact strongly with the fluorinated aggregates cores through the intermolecular hydrogen bonding.

Hence, the molecular motions of the nanoparticles would be remarkably restricted, and an extraordinarily enhanced light absorption would be observed in the carboxy-type fluorescein nanoparticles. Under such specific conditions, fluoresceins with only enol-form, especially carboxy-type tautomer possessing –OH and –C(=O)OH groups (see Fig. 10) could interact strongly with fluorinated aggregates cores through the intermolecular hydrogen bonding to afford fluorinated nanocomposites. In

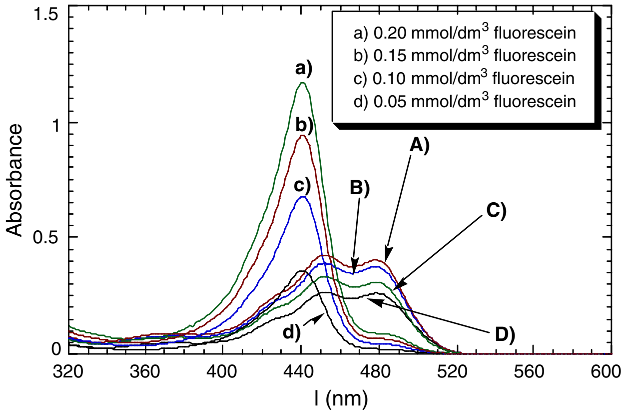

Fig. 8 Change of absorption spectra of fluorescein in the presence of R_F–(ACA)$_n$–R_F; R_F = $CF(CF_3)OC_3F_7$ (Mn = 5,220) in methanol at 30 °C concentration of R_F–(ACA)$_n$–R_F: 1.5 g/dm^3. In the absence of oligomer: (**A**) 0.20 mmol/dm^3 fluorescein, (**B**) 0.15 mmol/dm^3 fluorescein, (**C**) 0.10 mmol/dm^3 fluorescein and (**D**) 0.05 mmol/dm^3 fluorescein

Table 4 Association Number (n) of Fluorescein in the Presence of R_F–(ACA)$_n$–R_F [R_F = $CF(CF_3)OC_3F_7$] at 30 °C

Concentration of oligomer (g/dm^3)	n
1.5	0.8
0.9	0.7
0.6	0.8
0.3	0.9

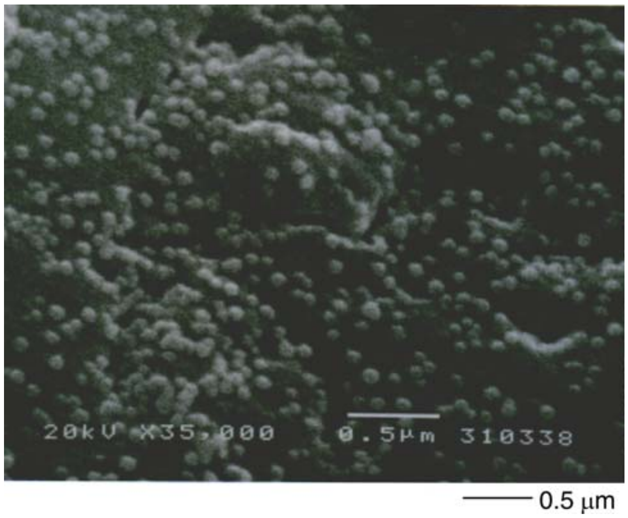

Fig. 9 SEM (scanning electron microscopy) images of methanol solution of R_F–(DOBAA)$_n$–R_F [R_F = $CF(CF_3)OC_3F_7$; 2 g/dm^3] and fluorescein (0.1 mmol/dm^3)

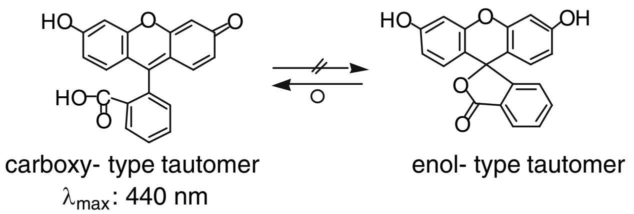

Fig. 10 Carboxy-type Tautomer and enol-type tautomer of fluorescein

fact, the ZINDO molecular orbital theoretical studies (programs: Gaussian 03W) [12] suggested that the carboxy-type tautomer in Fig. 10 could absorb the light effectively through the HOMO-LUMO (π–π^* transition) interaction to exhibit the absorption at $\lambda_{\max}$: 412 nm (theoretical) [experimental $\lambda_{\max}$: 437 nm (see Ref. [13]) owing to the higher flatness of this tautomer]. The molecular motions of fluoresceins in the nanocomposites would be remarkably restricted, and an extraordinarily enhanced light absorption would be observed in the carboxy-type fluorescein nanocomposites. A similar light absorption behavior was observed in the case of naphthofluorescein, indicating that since this compound possesses the same functional groups such as carboxyl, hydroxyl and carbonyl (quinone unit) groups as with fluorescein carboxy-type tautomer, naphthofluorescein should interact tightly with fluorinated aggregate cores through the intermolecular hydrogen bonding to afford fluorinated oligomer/naphthofluorescein nanocomposites.

Conclusion

Self-assembled oligomeric aggregates formed by fluoroalkyl end-capped DOBAA, DMAA, and ACA oligomers could provide suitable host moieties to interact with fluoresceins and naphthofluoresceins as guest molecules. These fluorinated oligomers/fluoresceins and naphthofluorescein nanocomposites thus obtained afforded an extremely enhanced light absorption around 440 and 520 nm, respectively; however, the corresponding non-fluorinated oligomers cannot afford such absorption bands at all under similar conditions. The enhanced narrow absorption band around 440 nm was not observed in the presence of fluoroalkyl end-capped 2-carboxyethy acrylate oligomers, although fluoroalkyl end-capped acrylic acid oligomers could afford this enhanced absorption. This finding suggests that the formation of the self-assembled fluorinated oligomeric aggregate cores are essential for the observation of these enhanced narrow absorptions. Especially, it was demonstrated that carboxyl and hydroxyl groups in fluorescein carboxy-type tautomer and naphthofluorescein should interact tightly with fluorinated aggregate cores through the intermolecular hydrogen bonding to afford fluorinated nanocomposites with an enhanced light absorption ability. Thus, these fluorinated fluorescein and naphthofluorescein nanocomposites have high potential to apply into a variety of fields including the recording materials.

Acknowledgements Thanks are due to Kohjin Co., Ltd. and Kyowa Hakko Kogyou Co., Ltd. for supply of DMAA and DOBAA, respectively. The authors also thank Dr. T. Saitoh of Waseda Junior and Senior High School (Tokyo, Japan) for helpful discussion on the ZINDO molecular orbital theoretical studies.

References

1. (a) Ameduri B, Boutevin B (2004) Well-architectured fluoropolymers: synthesis, properties and applications. Elsevier, Amsterdam, p 231; (b) Imae T (2003) Curr Opinion Colloid Interf Sci 8:307
2. (a) Andruzzi L, Chiellini E, Galli G, Li X, Seok SH, Ober CK (2002) J Mater Chem 12:1684; (b) Lacroix-Desmzes P, Delair T, Pichot D, Boutevin B (2000) J Polym Sci, Pt A, Polym Chem 38:3845; (c) Lebreton P, Ameduri B, Boutevin B, Corpart JM (2002) Macromol Chem Phys 203:522; (d) Monteiro MJ, Adamy MM, Leeuwen BJ, Van Herk AM, Destarac M (2005) Macromolecules 38:1538; (e) Ming W, Van de Grampel RD, Gildenpfemmig A, Snijder A, Brongersma HH, Van de Linde R, De With G (2003) Polym Mater Sci Eng 88:517
3. (a) Sawada H, Gong Y-F, Minoshima Y, Matsumoto T, Nakayama M, Kosugi M, Migita T (1992) J Chem Soc, Chem Commun 537; (b) Sawada H, Itoh N, Kawase T, Mitani M, Nakajima H, Nishida M, Moriya Y (1994) Langmuir 10:994; (c) Sawada H, Yoshino Y, Ikematsu Y, Kawase T (2000) Eur Polym J 26:231; (d) Sawada H, Kawase T, Ikematsu Y, Ishii Y, Oue M, Hayakawa Y (1996) Chem Commun 179
4. (a) Sawada H (1996) Chem Rev 96:1779; (b) Sawada H, Kawase T (2001) Kobunshi Ronbunshu 58:147; (c) Sawada H, Kawase T (2001) Kobunshi Ronbunshu 58:255; (d) Sawada H (2000) J Fluorine Chem 105:219
5. (a) Sawada H (2007) Prog Polym Sci 32:509; (b) Sawada H (2007) Polym J 39:637
6. (a) Gong X, Milic T, Xu C, Batteas JD, Drain CM (2002) J Am Chem Soc 124:14290; (b) Takahashi S, Miura H, Kasai H, Okada S, Oikawa H, Nakanishi H (2002) J Am Chem Soc 124:10944; (c) Fu H-B, Yao J-N (2001) J Am Chem Soc 123:1434
7. Sasazawa K, Yamada Y, Fujisawa A, Saitoh T, Ueno K, Oharu K, Sawada H (2005) Colloid Polym Sci 283:812
8. Sawada H, Yoshino Y, Kurachi M, Kawase T, Takishita K, Tanedani T (2000) Polymer 41:397
9. (a) Jelly EE (1936) Nature 138:1009; (b) Scheibe G (1936) Angew Chem 49:563
10. (a) Herz AH (1974) Photogr Sci Eng 18:323; (b) Makino S, Kanamaru N, Tanaka J (1980) Bull Chem Soc Jpn 53:3120
11. An B-K, Kwon S-Ki, Jung S-D, Park SY (2002) J Am Chem Soc 124:14410
12. This work was cited for the following program: Cite this work as: Gaussian 03W, Revision B.02, Frisch MJ, Trucks GW, Schlegel HB, Scuseria GE, Robb MA, Cheeseman JR, Montgomery JA Jr, Vreven T, Kudin KN, Burant JC, Millam JM, Iyengar SS, Tomasi J, Barone V, Mennucci B, Cossi M, Scalmani G, Rega N, Petersson GA, Nakatsuji H, Hada M, Ehara M, Toyota K, Fukuda R, Hasegawa J, Ishida M, Nakajima T, Honda Y, Kitao O,

Nakai H, Klene M, Li X, Knox JE, Hratchian HP, Cross JB, Adamo C, Jaramillo J, Gomperts R, Stratmann RE, Yazyev O, Austin AJ, Cammi R, Pomelli C, Ochterski JW, Ayala PY, Morokuma K, Voth GA, Salvador P, Dannenberg JJ, Zakrzewski VG, Dapprich S, Daniels AD, Strain MC, Farkas O, Malick DK, Rabuck AD, Raghavachari K, Foresman JB, Ortiz JV, Cui Q, Baboul AG, Clifford S, Cioslowski J, Stefanov BB, Liu G, Liashenko A, Piskorz P, Komaromi I, Martin RL, Fox DJ, Keith T, Al-Laham MA, Peng CY, Nanayakkara A, Challacombe M, Gill PMW, Johnson B, Chen W, Wong MW, Gonzalez C, Pople JA (2003) Gaussian, Inc., Pittsburgh PA

13. (a) Tamura Z, Morioka T, Maeda M, Tsuji A (1994) Bunseki Kagaku 43:339; (b) Chen S-C, Nakamura H, Tamura Z (1979) Chem Pharm Bull 27:475